Journal of Power Sources 236 (2013) 169–174

Contents lists available at SciVerse ScienceDirect

Journal of Power Sources

journal homepage: www.elsevier.com/locate/jpowsour

Short communication

Simply AlF_3-treated $Li_4Ti_5O_{12}$ composite anode materials for stable and ultrahigh power lithium-ion batteries

Wu Xu [a,*], Xilin Chen [a], Wei Wang [a], Daiwon Choi [a], Fei Ding [a,b], Jianming Zheng [a], Zimin Nie [a], Young Joon Choi [a], Ji-Guang Zhang [a,*], Z. Gary Yang [a,*,1]

[a] Energy and Environment Directorate, Pacific Northwest National Laboratory, Richland, WA 99354, United States
[b] National Key Lab of Power Sources, Tianjin Institute of Power Sources, Tianjin 300381, China

HIGHLIGHTS

- Commercial LTO is successfully modified by AlF_3 via a low temperature process.
- The composite consists of Al^{3+}/F^- co-doped LTO with trace anatase TiO_2.
- The doped LTO composite shows ultrahigh rate capability over the pristine LTO.
- It also delivers higher discharge capacity and maintains long-term cycling stability.

ARTICLE INFO

Article history:
Received 26 December 2012
Received in revised form
14 February 2013
Accepted 20 February 2013
Available online 28 February 2013

Keywords:
$Li_4Ti_5O_{12}$
AlF_3 treatment
Doping
Anode
Lithium-ion battery
High power

ABSTRACT

The commercial $Li_4Ti_5O_{12}$ (LTO) is successfully modified by AlF_3 via a low temperature process. After being calcined at 400 °C for 5 h, AlF_3 reacts with LTO to form a composite material which mainly consists of Al^{3+} and F^- co-doped LTO with small amounts of anatase TiO_2. Al^{3+} and F^- co-doped LTO demonstrates ultrahigh rate capability comparing to the pristine LTO. Since the amount of the byproduct TiO_2 is relatively small, the modified LTO electrodes retain the main voltage characteristics of LTO with a minor feature similar to those of anatase TiO_2. The doped LTO anodes deliver slightly higher discharge capacity and maintain the excellent long-term cycling stability when compared to the pristine LTO anode. Therefore, Al^{3+} and F^- co-doped LTO composite material synthesized at low temperature is an excellent anode for stable and ultra-high power lithium-ion batteries.

1. Introduction

$Li_4Ti_5O_{12}$ (LTO) spinel has been regarded as one of the most promising anode materials to replace graphite for large-scale lithium-ion batteries [1] because of its negligible volume change [2], flat potential around 1.55 V vs. Li/Li^+ during charge and discharge [2], no formation of SEI layer and metallic lithium, high safety, high thermal stability [3,4], and excellent cycle life within a wide operating temperature range [3]. However, the very low electronic conductivities of spinel LTO arising from the empty Ti 3d state with band energy of about 2–3 eV and the sluggish lithium ion diffusion in LTO result in the poor power performance of the LTO materials [5–7], preventing them from being widely used. Several approaches have been pursued over the past few years to improve the power performance of LTO. One way is to develop nano-sized particles [3,7,8] or porous particles [6,9–12] in order to reduce Li^+ diffusion paths and to provide large contact area between the electrode and electrolyte. Another is to improve the electrical conductivity of the active materials by doping with cations [13–18] and anions [19–21], to modify the surface with carbon coating [11,22–26], and to form composites with carbon, metals or metal oxides [27–32].

Doping of Al^{3+} or F^- to promote the rate capability of LTO has recently been reported [15,16,21], and some good results were achieved. However, the co-doping of Al^{3+} and F^- to LTO was not

* Corresponding authors. Tel.: +1 509 375 6934; fax: +1 509 375 2186.
E-mail addresses: wu.xu@pnnl.gov (W. Xu), jiguang.zhang@pnnl.gov (J.-G. Zhang), gary.yang@uetechnologies.com (Z.G. Yang).
[1] Present address: UniEnergy Technologies, LLC, 4333 Harbour Pointe Blvd. SW, Unit A, Mukilteo, WA 98275, United States. Tel.: +1 425 290 8898; fax: +1 425 740 9898.

0378-7753/$ – see front matter © 2013 Elsevier B.V. All rights reserved.
http://dx.doi.org/10.1016/j.jpowsour.2013.02.055

successful [33]. Huang et al. reported Al^{3+} and F^- co-substituted compounds $Li_4Al_xTi_{5-x}F_yO_{12-y}$ via a solid-state reaction method at high temperature (900 °C) [33] but the performance is even worse than that of the pristine LTO. The reason is probably the loss of partial lithium and fluorine during the preparation process at high temperatures.

In this paper, we report a simple method to make Al^{3+} and F^- co-doped LTO composite anode materials via a low-temperature reaction between LTO and AlF_3. Since the processing temperature is as low as 400 °C, the volatilization of lithium and fluorine is effectively avoided. The materials are characterized and their excellent rate capability and cycling stability are discussed.

2. Experimental

The AlF_3-treated LTO samples were prepared following the procedures described in literature for AlF_3-coated cathode materials and graphite [34,35]. Commercial LTO powders (nanopowder, 22-nm particle size, ≥98% trace metal basis, Sigma–Aldrich) were used for the study. Aluminum nitrate nonahydrate (98+%, Sigma–Aldrich) and ammonium fluoride (98+%, Sigma–Aldrich) were added at a fixed stoichiometric molar ratio of $Al^{3+}/F^- = 3$ and at different amounts. After purification with deionized water, the solid powders were calcined in a tube furnace at 400 °C for 5 h with the continuous flowing of pure argon. The obtained AlF_3-modified LTO samples are denoted *m*AFLTO where *m* is the weight percentage of AlF_3 added on the basis of the LTO weight (i.e. $m = 1$ for 1%, and $m = 5$ for 5%).

The *m*AFLTO electrodes were prepared from the mixture of *m*AFLTO, Super P carbon black (from Timcal) and polyvinylidene fluoride (PVDF, Solef 5130, from Solvay) at 8:1:1 by weight. The Li|*m*AFLTO coin cells were assembled inside an MBraun glove box filled with purified argon with the electrolyte of 1.0 M $LiPF_6$ in ethylene carbonate-dimethyl carbonate at a 1:2 volume ratio from Novolyte Technologies. For comparison, LTO electrode and its half cells were also prepared.

The cycling performance was tested on an Arbin BT-2000 battery tester between 1.0 and 2.5 V vs. Li/Li^+. The cell resistance was measured by electrochemical impedance spectroscopy on a Solartron Electrochemical Station SI-1287 and a Solartron Frequency Analyzer SI-1255. The *m*AFLTO samples were characterized using X-ray diffraction (XRD) and scanning electron microscopy (SEM). XRD was measured on a Philips Xpert X-ray diffractometer with Cu Kα radiation at λ 1.54 Å, from 10° to 70° at a scanning rate of 0.02° per 10 s. SEM images were obtained on a JEOL 5900 Scanning Electron Microscope at a working distance of 12 mm and an accelerating voltage of 20 keV. Elemental composition of the sample was analyzed using energy dispersive X-ray spectroscopy (EDX) that attached to the microscope (Oxford, ISIS analysis system).

3. Results and discussion

3.1. Material characterization

Fig. 1a shows the XRD patterns of the *m*AFLTO ($m = 1, 2, 3, 5$) and the commercial LTO. All four samples show the major peaks of cubic LTO (JCPDS No. 26-1199). The *m*AFLTO samples also show extra peaks for anatase TiO_2 (XRD pattern of JCPDS 75-2553) which are marked with asterisks (*). The intensity of the anatase TiO_2 peaks increases with *m*, the amount of AlF_3 added during the material preparation. Such peaks are hardly seen when $m = 1$ and 2 mainly because the formed anatase TiO_2 is in too small amount to be detected. When carefully analyzing the extra XRD peak at about 25°(Fig. 1b), it is found that this peak is for anatase TiO_2 (25.2°) but not for AlF_3 whose peak should be located at 25.0 as demonstrated by the XRD pattern of AlF_3/LTO mixture after ball milling and calcining at 450 °C for 5 h shown in Fig. 1c.

The appearance of XRD peaks for anatase TiO_2 and the loss of peaks for AlF_3 give a strong indication that the Al^{3+} may have entered the Ti^{4+} sites in LTO, i.e. the AlF_3 does not physically cover the surface of LTO particles, but has chemically reacted with LTO to form Al^{3+} and F^- co-doped LTO materials. The reaction is suggested below, which indicates the formed material is a composite of $Li_{4+x-y}Ti_{5-x}Al_xO_{12-y}F_y$ and anatase TiO_2.

$$Li_4Ti_5O_{12} + AlF_3 \xrightarrow[5\ h]{400\ ^\circ C} TiO_2 + Li_{4+x-y}Ti_{5-x}Al_xO_{12-y}F_y \quad (1)$$

When comparing the XRD patterns of *m*AFLTO in this work and the Al^{3+}/F^- co-doped spinel compounds in Ref. [33], it is found that these materials are not identical especially for the intensity of peaks at 2θ of about 28.5° and 47.2° and for the loss of the peaks at 2θ of about 56.0° and 69.0° in *m*AFLTO materials. In addition, the reaction in this work occurs at a temperature much lower than the reported solid state reactions for preparation of doped LTO materials. In

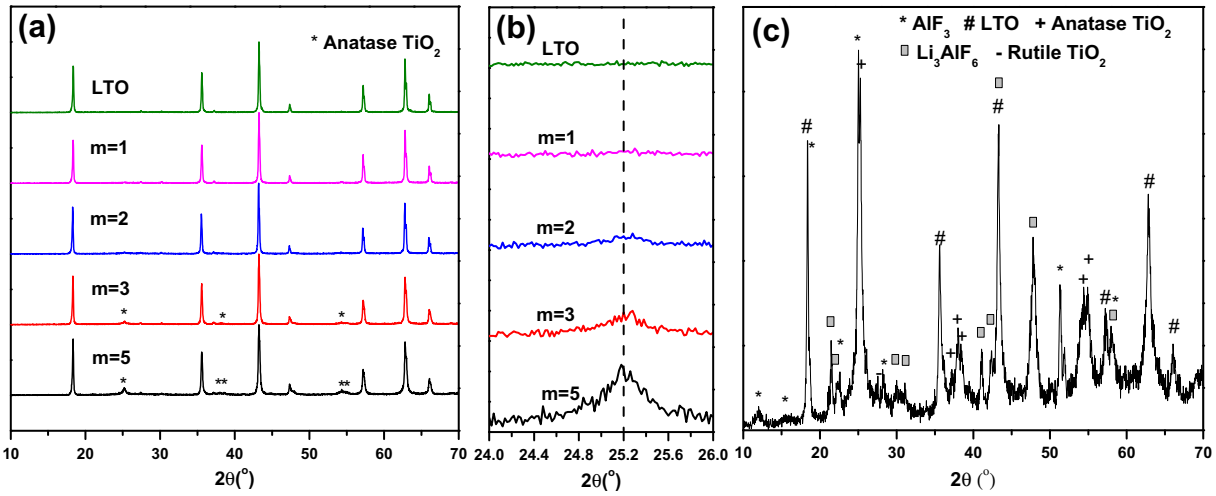

Fig. 1. (a) XRD patterns and enlarged peaks at (b) $2\theta = 24.0°–26.0°$ of pristine LTO and *m*AFLTO ($m = 1, 2, 3, 5$) composites; (c) XRD patterns of composites obtained by reacting LTO and AlF_3 at a 1:1 ratio in weight.

those high-temperature (i.e. 900 °C) reactions, severe loss of lithium and fluorine elements happens due to volatilization [33]. Therefore, the low-temperature reaction for Al^{3+} and F^- co-doping LTO can effectively avoid the volatile loss of Li and fluorine elements.

As shown in the SEM image and the EDX mapping of Al, F, O and Ti for *m*AFLTO samples (Fig. 2), all four elements are uniformly presented in the composite material, indicating the concomitant TiO_2 and $Li_{4+x-y}Ti_{5-x}Al_xO_{12-y}F_y$ are well distributed in the composite. These evidences suggest that the commercial LTO might be successfully doped by Al^{3+} and F^- via the low temperature reaction at 400 °C. However, the detailed analyses on the composite materials especially the distribution and doping sites of Al^{3+} and F^- in the materials, the exact doping amounts of Al^{3+} and F^-, and the effect of F^- doping on the ionic/electronic conductivities are currently under investigation.

3.2. Electrochemical behavior and battery performance

Fig. 3a–e shows the cyclic voltammetric curves of pristine LTO and *m*AFLTO ($m = 1, 2, 3, 5$) composites in the voltage range between 1.0 and 2.5 V at a scan rate of 10 μV s^{-1}. For pristine LTO (Fig. 3a), the reduction peak during the first cathodic scan is located at 1.43 V and the corresponding oxidation peak during the first anodic scan appears at 1.71 V. In the following scans, the reduction peak shifts to 1.50 V and splits into two peaks. The peak at 1.43 V shrinks and the peak at 1.50 V increases in following scans. In the meantime, the oxidation peak shifts to 1.68 V. No redox peaks are observed in the voltage range of 1.6–2.1 V (see the inset of Fig. 3a). The two split reduction peaks were reported previously [31] and is mainly related to the spinel/rock-salt two-phase transition reaction (2).

$$Li_4Ti_5O_{12} + 3Li^+ + 3e^- \leftrightarrow Li_7Ti_5O_{12} \quad (2)$$

Similar to the pristine LTO, the four *m*AFLTO composite materials all show the shift of the reduction peak from about 1.39–1.41 V to about 1.49–1.50 V accompanying two split peaks and the shift of the corresponding oxidation peak from 1.70–1.72 V to about 1.67–1.66 V, as seen in Fig. 3b–e. Beyond this similarity, all doped composites also exhibit an extra pair of redox peak in the voltage range between 1.6 and 2.1 V (the insets of Fig. 3b–e) and the current response of this redox reaction increases with the anatase TiO_2, a concomitant product in reaction (1). Its reduction peak shifts from 1.71 V to 1.74 V after the initial cathodic scans and the corresponding oxidation peak maintains at about 1.93 V. This extra pair of redox peak is ascribed to the Li^+ insertion into and de-insertion out of anatase TiO_2 [36,37]. The CV test results are consistent with the XRD analysis results.

The redox behavior of anatase TiO_2 in the *m*AFLTO composites and the contribution of TiO_2 to the total capacities can also be demonstrated in the voltage profiles of the *m*AFLTO composite materials. Fig. 3f compares the first cycle voltage profiles of Li^+ insertion (i.e. discharge process) and de-insertion (i.e. charge process) of the *m*AFLTO ($m = 1, 2, 3, 5$) and pristine LTO in half cells in the voltage range between 1.0 and 2.5 V at C/10 rate and at room temperature. The half cells of *m*AFLTO and the pristine LTO all demonstrate a long range of flat voltage at about 1.56–1.54 V during discharge and about 1.56–1.58 V during charge, which are assigned to the Li^+ insertion and de-insertion of the two-phase reaction (2) and are also corresponding to the one pair of strong redox peaks in the CV scans shown in Fig. 3a–e. As for the *m*AFLTO ($m = 1, 2, 3, 5$) composite materials, with the *m* increasing from 1 to 5, the small voltage plateaus at ~1.7 V during discharge and ~1.9 V during charge extend steadily. As discussed above, these small plateaus correspond to the Li^+ insertion and de-insertion of the formed anatase TiO_2, thus it is indicated that the capacities contributed by TiO_2 increase with increasing *m* values. In addition, all *m*AFLTO samples except for 5AFLTO deliver slightly higher total capacities than the pristine LTO does during both discharge and charge processes. It indicates that Al^{3+} and F^- co-doping increases the reversible capacity of LTO in a certain amount of AlF_3 usage in the composite preparation. However, only 1AFLTO delivers higher Li-de-insertion capacity than the pristine LTO in the voltage range from 1.5 V to 1.6 V where the capacity is solely contributed by LTO or $Li_{4+x-y}Ti_{5-x}Al_xO_{12-y}F_y$. Too much doping may result in ionic conductivity decrease as well as total conductivity decrease though the electronic conductivity increase slightly [16]. The improvement of reversible capacity in 1AFLTO is clearly caused by the improvement of total conductivity of LTO after Al^{3+} and F^- doping. Since 1AFLTO has little capacity from TiO_2, it will be used for further evaluation and comparison with commercial LTO.

It has been reported that Al^{3+} doping can enhance the electronic conductivity of LTO [16,33] and F^- doping can effectively improve the electrochemical performance of LTO [21] and TiO_2 [38]. Thus it is reasonable to believe that the Al^{3+} and F^- co-doping can improve the rate capability of LTO. Fig. 4a shows the rate capability with cycling of the pristine LTO and the 1AFLTO at room temperature. The specific capacities of Li de-insertion for 1AFLTO are 173, 169,

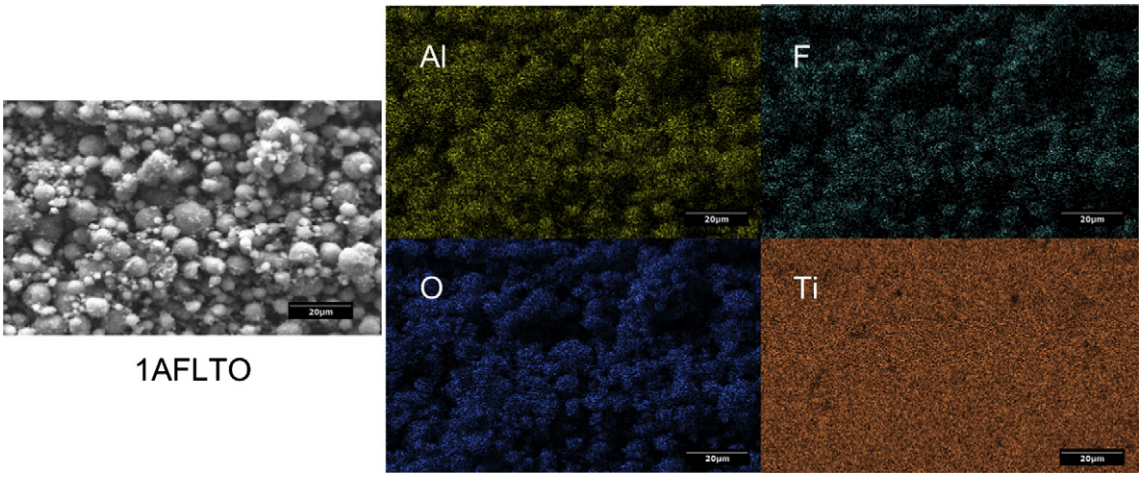

Fig. 2. Scanning electron microscopic image and elemental mapping of 1AFLTO clearly shows the uniform distribution of aluminum and fluorine elements in the AFLTO composite.

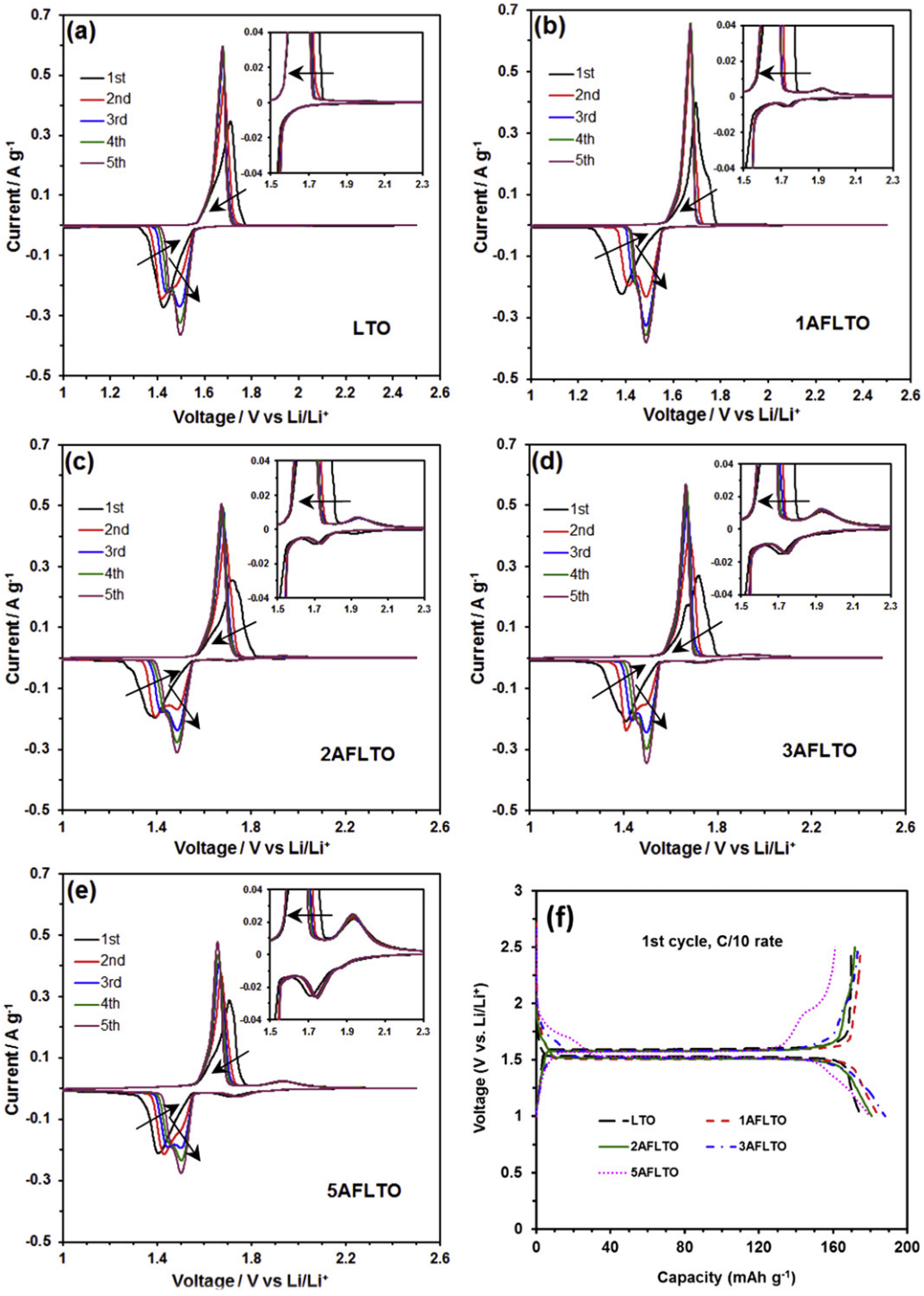

Fig. 3. (a)–(e) Cyclic voltammograms of *m*AFLTO (m = 0, 1, 2, 3, 5); (f) the galvanostatic charge–discharge curve of pristine LTO and *m*AFLTO composites at C/10 and room temperature. (Arrows point from 1st to 5th)

162, 160, 155, 143 and 106 mAh g^{-1} at C/5, 1C, 5C, 10C, 20C, 30C and 50C rate, respectively, while those for the pristine LTO are 169, 165, 159, 152, 133, 88 and 39 mAh g^{-1} at C/5, 1C, 5C, 10C, 20C, 30C and 50C rate, respectively. The superior rate performance of 1AFLTO originates from the high total conductivity of the electrode composites, evidenced by the impedance results as shown in Fig. 4b. The solid lines in Fig. 4b were fitted by the equivalent circuit as inserted in Fig. 4b. The Nyquist plots for both LTO and 1AFLTO consist of two depressed semicircles in the high to medium frequency range and an infinite diffusion line in the low frequency range. From the fitted data, the resistance of electrolyte (R_{el}, about 2 Ω) and the resistance of solid electrolyte interphase film (R_{sei}, about 7 Ω) are similar for both 1AFLTO and the pristine LTO. However, the charge transfer resistance (R_{ct}) of 1AFLTO (61 Ω) is smaller than that of the pristine LTO (71 Ω). The decrease in the charge transfer resistance may be caused by the smaller particle

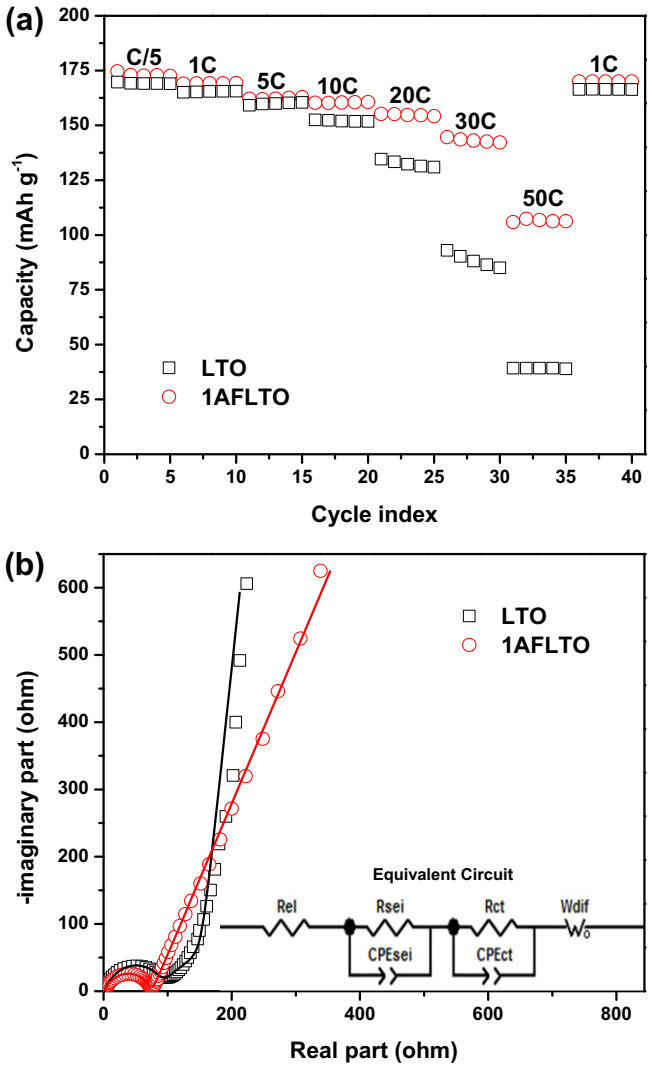

Fig. 4. (a) Capacity retention at different C-rates (1C = 175 mAh g^{-1}) and (b) impedance after being fully charged at C/5 of pristine LTO and 1AFLTO at room temperature (solid lines are for fitted data).

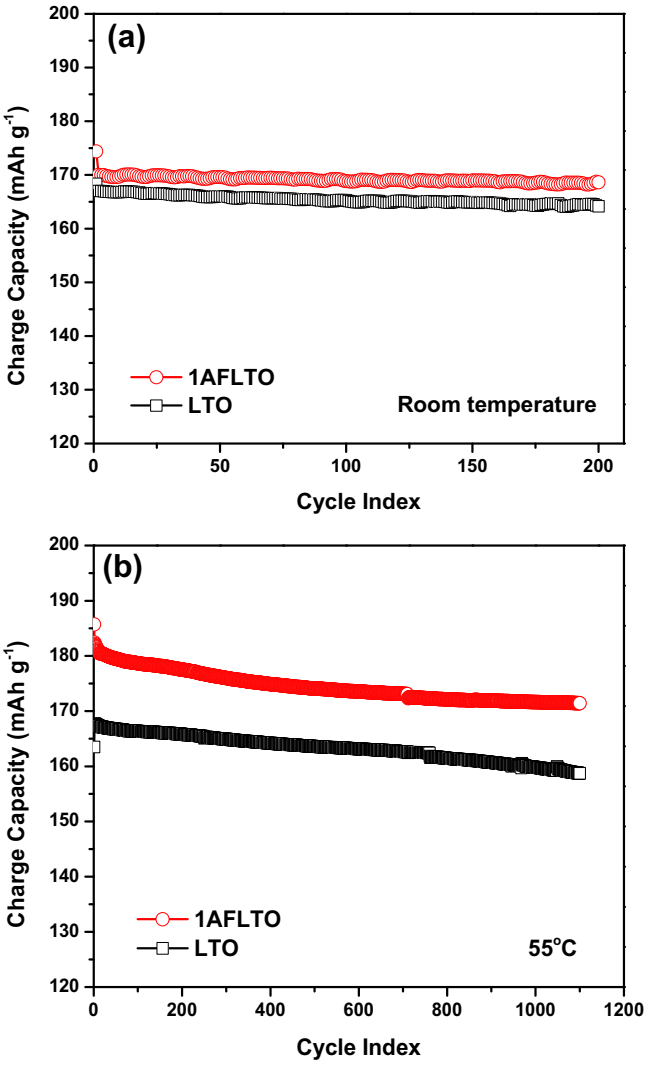

Fig. 5. Cycling performance of pristine LTO and 1AFLTO at room temperature (a) and 55 °C (b).

size in 1AFLTO since the *in-situ* generated TiO_2 limited the growth of LTO particles, leading to higher surface area or higher exchange current density [39]. Based on the values of the fitted Warburg element, the ionic diffusion coefficient in 1AFLTO is almost four times of that in pristine LTO. It is indicated that 1AFLTO has much higher ionic conductivity than the pristine LTO. The reason can be explained as below: Besides the improvement of both ionic and electronic conductivities of the commercial LTO by co-doping of Al^{3+} and F^- elements, the *in-situ* generated TiO_2 enhance the ionic diffusion in the electrode by restraining growth of LTO particles [32] and providing short ionic diffusion path through the boundary among TiO_2 and LTO [30,40]. Considering all these factors, the *m*AFLTO composites with appropriate *m* values exhibit superior rate performance than the pristine LTO.

The improvement of rate capability is not at the cost of the stability. In fact, the stability has been maintained when the cycling is conducted at both room temperature and elevated temperatures. The long-term cycling performance at 1C rate of the pristine LTO and 1AFLTO at room temperature and 55 °C are plotted in Fig. 5a and b, respectively. When cycled at room temperature, the 1AFLTO delivers slightly higher capacity during prolonged cycling test. The pristine LTO shows the de-insertion capacity of 167.0 and 164.2 mAh g^{-1} at the second and 200th cycles, respectively, with a capacity loss of 0.008% per cycle, while the 1AFLTO shows the de-insertion capacity of 170.0 and 168.6 mAh g^{-1} at the same cycles, with a capacity loss of 0.004% per cycle (after the first cycle). As for the cycling stability at 1C rate and high temperature (55 °C), the pristine LTO has the de-insertion capacity of 167.7 and 158.7 mAh g^{-1} at the second and 1100th cycles, with a capacity loss of 0.005% per cycle, while the 1AFLTO demonstrated 182.4 and 171.4 mAh g^{-1} at the same cycle numbers, with a capacity loss of 0.005% per cycle. If looking into the capacity loss after the 800th cycle, the capacity loss per cycle is only 0.001% for 1AFLTO, significantly lower than 0.006% for the pristine LTO. This might be an evidence that the F^- substitution does help to stabilize LTO in the long-term cycling at 55 °C since the F^- doping may protect the electrode materials from corrosion by strong acid HF and strong Lewis acids PF_5 and POF_3 that are usually presented in $LiPF_6$-based electrolytes due to the hydrolysis and decomposition of $LiPF_6$ [35].

4. Conclusion

A low-temperature process was developed to make ultrahigh power LTO composite materials via the reaction between AlF_3 and

LTO. The commercial LTO particles can be co-doped with both Al^{3+} and F^- and simultaneously form a composite with the *in-situ* generated anatase TiO_2. The composite materials with appropriate doping amount exhibit significantly improved high-rate capability because both cation (Al^{3+}) and anion (F^-) doping increase the electronic conductivity. The capacity of doped LTO can be as high as 100 mAh g^{-1} at 50C rate and room temperature, corresponding to 57.1% capacity retention. The F^- doping also protects LTO from the attack of acidic species in $LiPF_6$-electrolytes thus enhances its long-term cycling stability. It is therefore believed that Al^{3+} and F^- co-doped LTO composite materials are excellent anodes for stable and ultrahigh power lithium-ion batteries.

Acknowledgment

This work was supported by the Assistant Secretary for Energy Efficiency and Renewable Energy, Office of Vehicle Technology of the U.S. Department of Energy.

References

[1] K. Ariyoshi, T. Hozuku, J. Power Sources 174 (2007) 1258.
[2] T. Ohzuku, A. Ueda, N. Yamamoto, J. Electrochem. Soc. 142 (1995) 1431.
[3] K. Amine, I. Belharouak, Z. Chen, T. Tran, H. Yumoto, N. Ota, S.-T. Myung, Y.-K. Sun, Adv. Mater. 22 (2010) 3052.
[4] K. Zaghib, M. Armand, M. Gauthier, J. Electrochem. Soc. 145 (1998) 3135.
[5] C.Y. Ouyang, Z.Y. Zhong, M.S. Lei, Electrochem. Commun. 9 (2007) 1107.
[6] K.-C. Hsiao, S.-C. Liao, J.-M. Chen, Electrochim. Acta 53 (2008) 7242.
[7] A.S. Prakash, P. Manikandan, K. Ramesha, M. Sathiya, J.-M. Tarascon, A.K. Shukla, Chem. Mater. 22 (2010) 2857.
[8] S.C. Lee, S.M. Lee, J.W. Lee, J.B. Lee, S.M. Lee, S.S. Han, H.C. Lee, H.J. Kim, J. Phys. Chem. C 113 (2009) 18420.
[9] E.M. Sorensen, S.J. Barry, H.-K. Jung, J.R. Rondinelli, J.T. Vaughey, K.R. Poeppelmeier, Chem. Mater. 18 (2006) 482.
[10] C. Jiang, Y. Zhou, I. Honma, T. Kudo, H. Zhou, J. Power Sources 166 (2007) 514.
[11] L. Shen, C. Yuan, H. Luo, X. Zhang, L. Chen, H. Li, J. Mater. Chem. 21 (2011) 14414.
[12] J. Chen, L. Yang, S. Fang, S. Hirano, K. Tachibana, J. Power Sources 200 (2012) 59.
[13] C.H. Chen, J.T. Vaughey, A.N. Jansen, D.W. Dee, A.J. Kahaian, T. Goacher, M.M. Thackeray, J. Electrochem. Soc. 148 (2001) A102.
[14] S. Huang, Z. Wen, X. Zhu, Z. Gu, Electrochem. Commun. 6 (2004) 1093.
[15] S. Huang, Z. Wen, X. Zhu, Z. Lin, J. Power Sources 165 (2007) 408.
[16] H. Zhao, Y. Li, Z. Zhu, J. Lin, Z. Tian, R. Wang, Electrochim. Acta 53 (2008) 7079.
[17] D. Capsoni, M. Bini, V. Massarotti, P. Mustarelli, S. Ferrari, G. Chiodelli, M.C. Mozzati, P. Galinetto, J. Phys. Chem. C 113 (2009) 19664.
[18] R. Cai, S. Jiang, X. Yu, B. Zhao, H. Wang, Z. Shao, J. Mater. Chem. 22 (2012) 8013.
[19] K.-S. Park, A. Benayad, D.-J. Kang, S.-G. Doo, J. Am. Chem. Soc. 130 (2008) 14930.
[20] Y. Qi, Y. Huang, D. Jia, S.-J. Bao, Z.P. Guo, Electrochim. Acta 54 (2009) 4772.
[21] H.-G. Jung, C.S. Yoon, J. Parkash, Y.-K. Sun, J. Phys. Chem. C 113 (2009) 21258.
[22] G.J. Wang, J. Gao, L.J. Fu, N.H. Zhao, Y.P. Wu, T. Takamura, J. Power Sources 174 (2007) 1109.
[23] T. Yuan, X. Yu, R. Cai, Y. Zhou, Z. Shao, J. Power Sources 195 (2010) 4997.
[24] H.-G. Jung, S.-T. Myung, C.S. Yoon, S.-B. Son, K.H. Oh, K. Amine, B. Scrosati, Y.-K. Sun, Energy Environ. Sci. 4 (2011) 1345.
[25] L. Zhao, Y.-S. Hu, H. Li, Z. Wang, L. Chen, Adv. Mater. 23 (2011) 1385.
[26] H.-G. Jung, J. Kim, B. Scrosati, Y.-K. Kim, J. Power Sources 196 (2011) 7763.
[27] H. Xiang, B. Tian, P. Lian, Z. Li, H. Wang, J. Alloys Compd. 509 (2011) 7205.
[28] S. Huang, Z. Wen, J. Zhang, X. Yang, Electrochim. Acta 52 (2007) 3704.
[29] S. Huang, Z. Wen, X. Zhu, X. Yang, J. Electrochem. Soc. 152 (2005) A1301.
[30] M.M. Rahman, J.-Z. Wang, M.F. Hassan, D. Wexler, H.K. Liu, Adv. Energy Mater. 1 (2011) 212.
[31] K.M. Kim, K.-Y. Kang, S. Kim, Y.-G. Lee, Curr. Appl. Phys. 12 (2012) 1199.
[32] J. Wang, H. Zhao, Q. Yang, C. Wang, P. Lv, Q. Xia, J. Power Sources 222 (2013) 196.
[33] S. Huang, Z. Wen, Z. Gu, X. Zhu, Electrochim. Acta 50 (2005) 4057.
[34] Y.-K. Sun, J.-M. Han, S.-T. Myung, S.-W. Lee, K. Amine, Electrochem. Commun. 8 (2006) 821.
[35] F. Ding, W. Xu, D. Choi, W. Wang, X. Li, M.H. Engelhard, X. Chen, Z. Yang, J.-G. Zhang, J. Mater. Chem. 22 (2012) 12745.
[36] K. Gerasopoulos, X. Chen, J. Culver, C. Wang, R. Ghodssi, Chem. Commun. 46 (2012) 7349.
[37] B. Zhao, Z. Shao, J. Phys. Chem. C 116 (2012) 17440.
[38] C.T. Cherian, M.V. Reddy, T. Magdaleno, C.-H. Sow, K.V. Ramanujachary, G.V. Subba Rao, B.V.R. Chowdari, CrystEngComm 14 (2012) 978.
[39] M. Mohamedi, D. Takahashi, T. Uchiyama, T. Itoh, M. Nishizawa, I. Uchida, J. Power Sources 93 (2001) 93.
[40] R. Miyazaki, H. Maekawa, ECS Electrochem. Lett. 1 (2012) A87.